

Supplementary Material

Cracking-oxidation of dibutyl phthlate: core-shell catalyst, decarboxylation mechanism, and process cost

Guoqing Zhang^a, Tao Wei^a, Shangpu Zhuang^a, Jihai Tang^a, Mifen Cui^a, Xu Qiao^a, Zhuxiu Zhang^{a}*

^aState Key Laboratory of Materials-Oriented Chemical Engineering, College of Chemical Engineering, Nanjing Tech University, No. 30 Puzhunan Road, Nanjing 211816, China

**Corresponding author. Tel.: +86 25 83587168; E-mail:*

zhuxiu.zhang@njtech.edu.cn

Content

Instrument analysis methods.	3
Fig. S1 Pore size distribution of Si-ZSM-5, CeO ₂ /Si-ZSM-5, Si-ZSM-5@Al-MS and CeO ₂ /Si-ZSM-5@Al-MS.	3
Fig. S2 DBP molecule structure (a), phthalic acid molecule structure (b), phthalic anhydride molecule structure (c), n-butanol molecule structure (d).	4
Fig. S3 Time-resolved the in-situ DRIFTS of in the flow of phthalic anhydride (a), benzene (b), n-butanol (c), n-butene (d) over CeO ₂ /Si-ZSM-5@Al-MS at 350 °C.	4
Fig. S4 Long-term stability evaluation at 350 °C and a space velocity of 20,000 h ⁻¹ of CuO@Hol-HZSM-5 catalyst.	5
Table S1 Properties of the catalysts.	5
Table S2 Acidities of the respective samples evaluated by Py-IR.	5
Table S3 The Fukin index of DBP.	6
Table S4 The Fukin index of phthalic acid.	7
Table S5 The Fukin index of phthalic anhydride.	7
Table S6 The Fukin index of n-butanol.	8
Table S7 The energy requirement, recovery of the adsorption thermal-desorption cracking-oxidation process.	8
Table S8 Comparison between adsorption thermal-desorption cracking-oxidation method and other methods.	9
Cost calculation equation.	9

Instrument analysis methods.

Transmission electron microscopy (TEM) and energy-dispersive X-ray spectroscopy (EDX) mapping analyses were performed on a JEOL JEM-2100F microscope equipped with a Bruker XFlash5030T detector. Scanning electron microscopy (SEM) images were acquired using a Phenom Pharos G2 benchtop field-emission scanning electron microscope (FE-SEM). Powder X-ray diffraction (PXRD) patterns were recorded on a Rigaku MiniFlex600 diffractometer operated at 40 kV and 15 mA. Nitrogen sorption isotherms were measured at 77 K using a Micromeritics 3Flex instrument. Hydrogen temperature-programmed reduction (H_2 -TPR) and ammonia temperature-programmed desorption (NH_3 -TPD) experiments were conducted using an AutoChem 2920 instrument. For H_2 -TPR analysis, the catalyst sample was first pretreated in an Ar flow at 300 °C for 1 h, cooled to 50 °C, and then heated from 50 to 600 °C under a 10 vol% H_2 /Ar flow while monitoring hydrogen consumption with a thermal conductivity detector (TCD). In the NH_3 -TPD experiments, the catalyst was pretreated in a He flow at 300 °C for 1 h, cooled to 50 °C, saturated with a 10 vol% NH_3 /He mixture, and subsequently heated from 50 to 600 °C under He, with the desorbed NH_3 monitored by TCD. X-ray photoelectron spectroscopy (XPS) analysis was performed on an ESCALAB 250Xi spectrometer operated at 40 kV and 40 mA under ultra-high vacuum ($<1 \times 10^{-7}$ Pa). The acidic properties of the synthesized catalysts were determined by pyridine adsorption Fourier transform infrared (FTIR) spectroscopy using a Nicolet iS50 FTIR spectrometer.

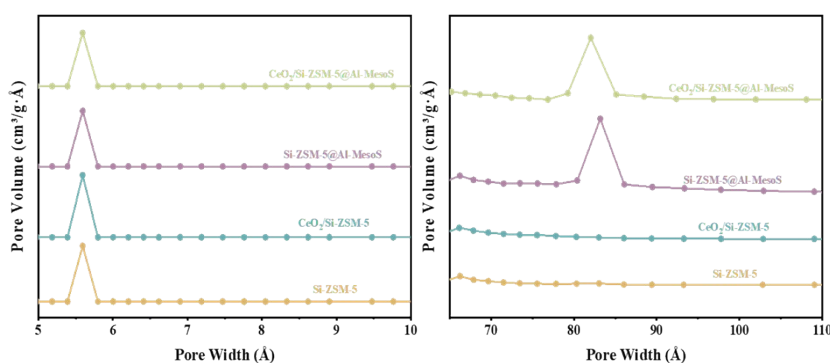


Fig. S1 Pore size distribution of Si-ZSM-5, CeO₂/Si-ZSM-5, Si-ZSM-5@Al-MS and CeO₂/Si-ZSM-5@Al-MS.

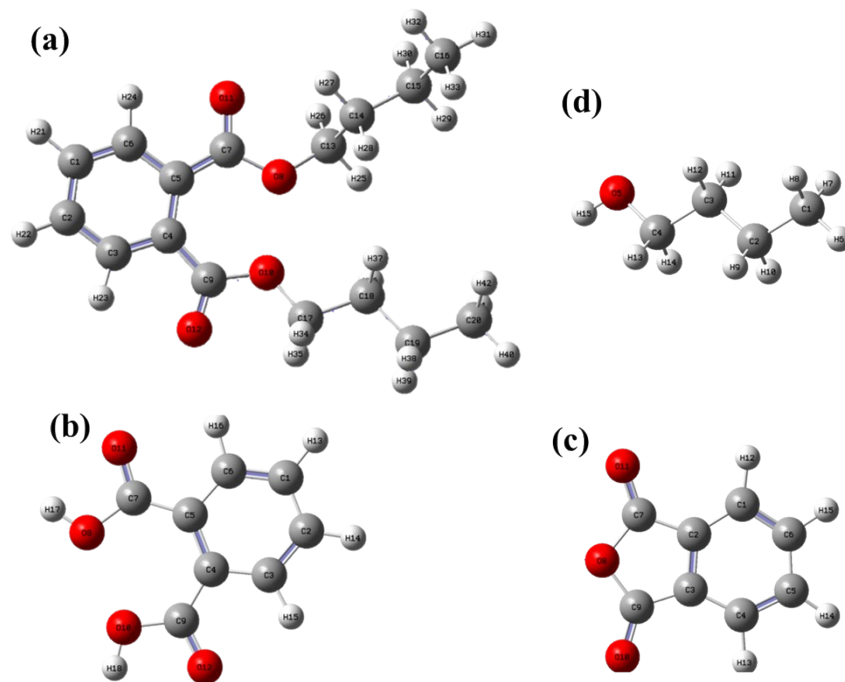


Fig. S2 DBP molecule structure (a), phthalic acid molecule structure (b), phthalic anhydride molecule structure (c), n-butanol molecule structure (d).

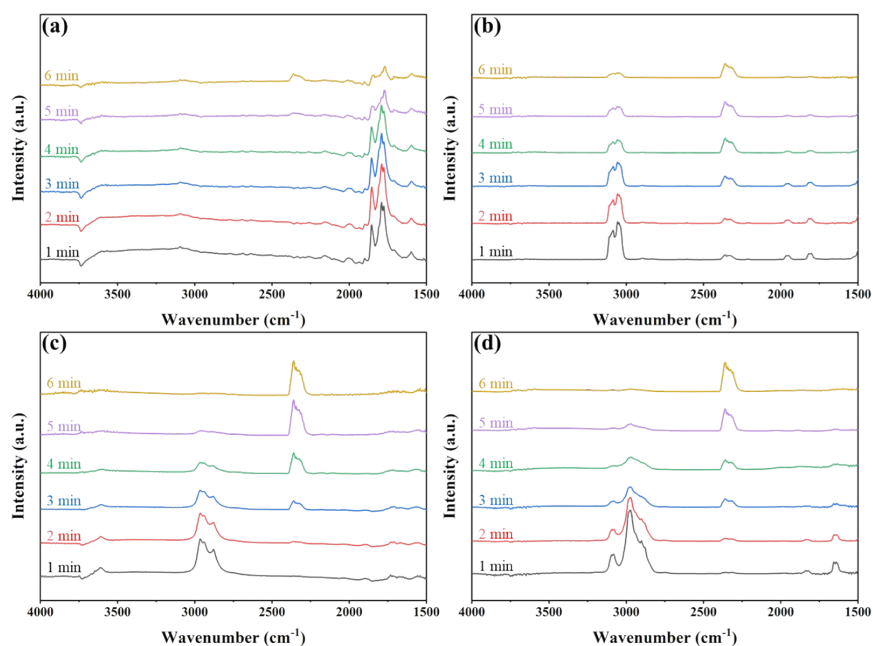


Fig. S3 Time-resolved the in-situ DRIFTS of in the flow of phthalic anhydride (a), benzene (b), n-butanol (c), n-butene (d) over CeO₂/Si-ZSM-5@Al-MS at 350 °C.

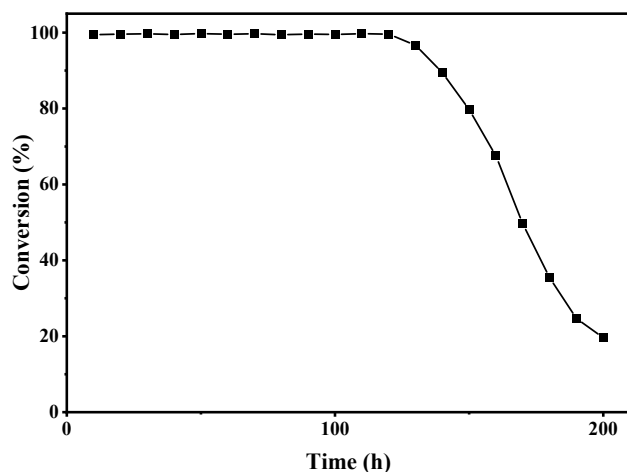


Fig. S4 Long-term stability evaluation at 350 °C and a space velocity of 20,000 h⁻¹ of CuO@Hol-HZSM-5 catalyst.

Table S1 Properties of the catalysts.

Catalysts	S _{BET} (m ² /g)	Pore volume (cm ³ /g)	Pore size (nm)
Si-ZSM-5	162.03	0.16	0.58
CeO ₂ /Si-ZSM-5	158.68	0.16	0.57
Si-ZSM-5@Al-MS	669.37	1.14	8.35
CeO ₂ /Si-ZSM-5@Al-MS	664.72	1.12	8.25

Table S2 Acidities of the respective samples evaluated by Py-IR.

Samples	Acidity types (mmol/g)			
	Brønsted		Lewis	
	200°C	350°C	200°C	350°C
Si-ZSM-5	0	0	trace	0
CeO ₂ /Si-ZSM-5	0	0	0.05	0.03
Si-ZSM-5@Al-MS	0.17	0.10	0.06	0.04
CeO ₂ /Si-ZSM-5@Al-MS	0.15	0.09	0.12	0.09

Table S3 The Fukin index of DBP

atom	q(N)	q(N+1)	q(N-1)	f	f ⁺	f ⁰
1(C)	-0.22106	-0.14964	-0.2212	-0.00014	-0.07142	-0.03578
2(C)	-0.19039	-0.17621	-0.19362	-0.00323	-0.01418	-0.0087
3(C)	-0.18808	-0.21764	-0.19061	-0.00253	0.029553	0.013511
4(C)	0.447616	0.449958	0.536715	0.089099	-0.00234	0.043379
5(C)	0.536746	0.390546	0.634105	0.097359	0.1462	0.12178
6(C)	-0.41839	-0.40773	-0.42737	-0.00898	-0.01066	-0.00982
7(C)	-0.04564	-0.26297	-0.05279	-0.00715	0.217334	0.10509
8(O)	-0.29356	-0.18868	-0.23221	0.061343	-0.10488	-0.02177
9(C)	0.374788	0.055976	0.372075	-0.00271	0.318812	0.15805
10(O)	-0.35453	-0.22211	-0.28736	0.067174	-0.13242	-0.03262
11(O)	-0.43727	-0.52345	-0.25846	0.178813	0.086175	0.132494
12(O)	-0.44289	-0.53494	-0.25788	0.185006	0.092054	0.13853
13(C)	-0.09554	-0.1412	-0.08456	0.010983	0.045657	0.02832
14(C)	-0.00574	0.22305	-0.04959	-0.04385	-0.22879	-0.13632
15(C)	-0.18116	-0.37204	-0.15455	0.026601	0.190883	0.108742
16(C)	-0.67785	-0.62641	-0.65404	0.023801	-0.05144	-0.01382
17(C)	-0.29091	-0.36927	-0.30994	-0.01903	0.078364	0.029669
18(C)	0.125057	-0.08089	0.075629	-0.04943	0.205949	0.078261
19(C)	-0.43544	-0.16264	-0.43574	-0.0003	-0.27279	-0.13655
20(C)	-0.53875	-0.74083	-0.50332	0.035424	0.202086	0.118755
21(H)	0.121248	0.071033	0.159661	0.038413	0.050215	0.044314
22(H)	0.119795	0.075087	0.158203	0.038408	0.044708	0.041558
23(H)	0.186788	0.127344	0.195987	0.009199	0.059444	0.034322
24(H)	0.180899	0.132238	0.190192	0.009293	0.048661	0.028977
25(H)	0.185349	0.131984	0.205506	0.020157	0.053365	0.036761
26(H)	0.169945	0.182092	0.200468	0.030523	-0.01215	0.009188
27(H)	0.206299	0.189285	0.203461	-0.00284	0.017014	0.007088
28(H)	0.181826	0.007347	0.193483	0.011657	0.174479	0.093068
29(H)	0.128454	0.129751	0.142323	0.013869	-0.0013	0.006286
30(H)	0.137517	0.137425	0.150453	0.012936	9.2E-05	0.006514
31(H)	0.151664	0.132236	0.171426	0.019762	0.019428	0.019595
32(H)	0.145675	0.154614	0.152311	0.006636	-0.00894	-0.00115
33(H)	0.147485	0.152941	0.153278	0.005793	-0.00546	0.000169
34(H)	0.171235	0.166085	0.20223	0.030995	0.00515	0.018073
35(H)	0.168768	0.146448	0.200219	0.031451	0.02232	0.026886
36(H)	0.127671	0.253342	0.141764	0.014093	-0.12567	-0.05579
37(H)	0.072095	0.156892	0.08912	0.017025	-0.0848	-0.03389
38(H)	0.1347	0.130059	0.147828	0.013128	0.004641	0.008884
39(H)	0.140559	0.140968	0.154422	0.013863	-0.00041	0.006727
40(H)	0.156703	0.142877	0.177342	0.020639	0.013826	0.017233
41(H)	0.149266	0.153104	0.154335	0.005069	-0.00384	0.000616
42(H)	0.149043	0.143979	0.150716	0.001673	0.005064	0.003369

Table S4 The Fukin index of phthalic acid

atom	q(N)	q(N+1)	q(N-1)	f	f ⁺	f ⁰
1(C)	-0.13802	-0.15451	-0.17859	-0.04057	0.016492	-0.01204
2(C)	-0.13793	-0.1544	-0.17857	-0.04064	0.016468	-0.01209
3(C)	0.051221	0.099811	-0.01317	-0.06439	-0.04859	-0.05649
4(C)	-0.36497	-0.27271	-0.55124	-0.18628	-0.09226	-0.13927
5(C)	-0.36577	-0.27355	-0.5519	-0.18613	-0.09222	-0.13917
6(C)	0.051204	0.099807	-0.01324	-0.06445	-0.0486	-0.05652
7(C)	0.760176	0.725186	0.856162	0.095986	0.03499	0.065488
8(O)	-0.56598	-0.48764	-0.59918	-0.0332	-0.07835	-0.05577
9(C)	0.76005	0.725021	0.856098	0.096048	0.035029	0.065539
10(O)	-0.56586	-0.48757	-0.59905	-0.03319	-0.0783	-0.05574
11(O)	-0.48224	-0.25319	-0.61378	-0.13154	-0.22905	-0.1803
12(O)	-0.48222	-0.25322	-0.61373	-0.13151	-0.22899	-0.18025
13(H)	0.141986	0.190349	0.079826	-0.06216	-0.04836	-0.05526
14(H)	0.141985	0.190351	0.079822	-0.06216	-0.04837	-0.05526
15(H)	0.177502	0.198534	0.132994	-0.04451	-0.02103	-0.03277
16(H)	0.1775	0.198524	0.132994	-0.04451	-0.02102	-0.03277
17(H)	0.420687	0.454608	0.387285	-0.0334	-0.03392	-0.03366
18(H)	0.420678	0.454594	0.387276	-0.0334	-0.03392	-0.03366

Table S5 The Fukin index of phthalic anhydride

atom	q(N)	q(N+1)	q(N-1)	f	f ⁺	f ⁰
1(C)	-0.36243	-0.31776	-0.16851	0.193922	-0.04467	0.074627
2(C)	0.073779	-0.09621	0.113593	0.039814	0.169986	0.1049
3(C)	0.207414	-0.02575	0.095295	-0.11212	0.233161	0.060521
4(C)	-0.4742	-0.50937	-0.40324	0.070961	0.035169	0.053065
5(C)	-0.0226	0.161294	0.225853	0.248452	-0.18389	0.03228
6(C)	-0.11909	-0.20381	-0.10648	0.012611	0.084719	0.048665
7(C)	0.57881	0.703223	0.654457	0.075647	-0.12441	-0.02438
8(O)	-0.377	-0.43637	-0.30542	0.071582	0.059371	0.065477
9(C)	0.659081	0.715155	0.722859	0.063778	-0.05607	0.003852
10(O)	-0.50094	-0.66663	-0.30424	0.196697	0.165693	0.181195
11(O)	-0.48451	-0.64723	-0.27759	0.206926	0.162713	0.18482
12(H)	0.231861	0.119724	0.229515	-0.00235	0.112137	0.054896
13(H)	0.202738	0.079697	0.180676	-0.02206	0.123041	0.05049
14(H)	0.201873	0.073035	0.181248	-0.02063	0.128838	0.054107
15(H)	0.18522	0.051001	0.161984	-0.02324	0.134219	0.055492

Table S6 The Fukin index of n-butanol

atom	q(N)	q(N+1)	q(N-1)	f	f ⁺	f ⁰
1(C)	0.542553	-0.52538	1.361155	0.818602	1.067934	0.943268
2(C)	-0.1426	-0.11437	-2.50473	-2.36213	-0.02823	-1.19518
3(C)	-0.53965	-0.16461	-2.65542	-2.11577	-0.37504	-1.2454
4(C)	-0.11147	-0.08147	1.639601	1.751068	-0.02999	0.860538
5(O)	-0.24258	-0.37757	-0.28717	-0.04459	0.134995	-1.2454
6(H)	0.142323	0.195653	0.131186	-0.01114	-0.05333	-0.03223
7(H)	0.144931	0.192748	0.134913	-0.01002	-0.04782	-0.02892
8(H)	0.144919	0.19293	0.134889	-0.01003	-0.04801	-0.02902
9(H)	0.13571	0.178983	0.126319	-0.00939	-0.04327	-0.02633
10(H)	0.135735	0.179072	0.126321	-0.00941	-0.04334	-0.02638
11(H)	0.148195	0.195708	0.132872	-0.01532	-0.04751	-0.03142
12(H)	0.148152	0.195655	0.132852	-0.0153	-0.0475	-0.0314
13(H)	0.116773	0.252882	0.106279	-0.01049	-0.13611	-0.0733
14(H)	0.116812	0.253213	0.10619	-0.01062	-0.1364	-0.07351
15(H)	0.345301	0.426568	0.314735	-0.03057	-0.08127	-0.05592

Table S7 The energy requirement, recovery of the adsorption thermal-desorption cracking-oxidation process.

Medium	Temperature range (K)	Energy requirement (kJ)	Energy recovery process	Energy recovery (kJ)
H ₂ O	298-373	3,937.5	/	
	latent heat	28,250		
	373-623	6,562.5		
Air	298-623	188,611	Heat exchange 298 K-523 K	104,373.8
Activated carbon	298-423	23,625	/	
DBP	298-623	2,077.5	Reaction heat	84,305
Total energy consumption		253,063.5	Total energy recovery	104,373.8
Total energy input				64,384.7

Table S8 Comparison between adsorption thermal-desorption cracking-oxidation method and other methods.

Method	Pollutant	Conversion	Mineralization rate	Degradation time (h)	Secondary pollutants	Cost	Ref.
UVC/VUV-Fenton Oxidation	DMP	98.6%	62.8%	0.5	Sludge	28.24 \$/t	3
UV/persulfate	DBP	>90%	/	1		17.52 \$/t	4
Electro-peroxone	DEP	78.9%	/	1		22.43 \$/t	5
Fe(II)-MOFs@MIP/PS	DBP	97.1%	58.1%	>3		12.29 \$/t	6
Photodegradation	DMP, DOP	>60%	/	>3		24.29\$/t	7
Physical Adsorption	DBP, DMP	/	/	Continuous	Spent Activated Carbon	12.8 \$/t	8
Regenerative Thermal Oxidizer	VOCs	>99%	>99%	/	NOx · fly ahs	28.56 \$/t	9
Thermal desorption-cracking-oxidation	DEHP	>99%	>95%	Continuous	/	19.78 \$/t _{orbent}	10
Thermal desorption-cracking-oxidation	DBP	>99%	>95%	Continuous	/	0.13 \$/t	This research

Cost calculation equation

(1) The total energy for heating water:

$$\begin{aligned}
 Q_{H_2O} &= Q_{H_2O_{298K-373K}} + Q_{H_2O_{LH}} + Q_{H_2O_{373K-623K}} \\
 &= c_{H_2O} \times m_{H_2O} \times (373K - 298K) + r_{H_2O} \times m_{H_2O} + c_{H_2O_g} \times m_{H_2O} \times (623K - 373K) \\
 &= 38750 \text{ kJ}
 \end{aligned}$$

where c_{H_2O} is the specific heat capacity of water, m_{H_2O} is the mass of water, r_{H_2O} is the enthalpy of vaporization, $c_{H_2O_g}$ is the specific heat capacity of water vapor.

(2) The total energy for heating air:

$$\begin{aligned}
 Q_{air} &= Q_{air_{298K-623K}} \\
 &= c_{air} \times m_{air} \times (623K - 298K) = 188611 \text{ kJ}
 \end{aligned}$$

where c_{air} is the Where specific heat capacity of air, m_{air} is the mass of air.

(3) The energy for heating the activated carbon:

$$Q_{ac} = c_{ac} \times m_{ac} \times (423K - 298K) = 23625 \text{ kJ}$$

where c_{ac} is the specific heat capacity of the activated carbon, m_{ac} is the mass of the activated carbon.

(4) The energy for heating the DBP:

$$Q_{DBP} = c_{DBP} \times m_{DBP} \times (623K - 298K) = 2077.5 \text{ kJ}$$

Where c_{DBP} is the specific heat capacity of DBP, m_{DBP} is the mass of DBP.

(5) Reaction heat from DBP oxidation:

$$Q_{reaction\ heat} = m_{DBP} \div M_{DBP} \times \Delta H_{DBP}$$

$$= 84305 \text{ kJ}$$

where m_{DBP} is the mass of DBP, M_{DBP} is the molar mass of DBP, ΔH_{DBP} is the enthalpy change of DBP.

(6) Heat recovered from heat exchanger:

$$\begin{aligned} Q_{Heat\ exchange} &= c_{air} \times m_{air} \times (522 \text{ K} - 298 \text{ K}) \\ &= 104,373.8 \text{ kJ} \end{aligned}$$

where c_{air} is the specific heat capacity of air, m_{air} is the mass of air.

(7) Energy gap:

$$\begin{aligned} Q_{gap} &= Q_{H_2O} + Q_{air} + Q_{ac} + Q_{DBP} - Q_{reaction\ heat} - Q_{Heat\ exchange} \\ &= 64,384.7 \text{ kJ} \end{aligned}$$

References

1. Z. Dong, S. Li, E. R. Rene, X. Tan and W. Ma, *Chemosphere*, 2024, **352**, 141343.
2. Z. Wang, Y. Shao, N. Gao and N. An, *Sep. Purif. Technol.*, 2018, **195**, 92-100.
3. M. Hou, Y. Chu, X. Li, H. Wang, W. Yao, G. Yu, S. Murayama and Y. Wang, *J. Hazard. Mater.*, 2016, **319**, 61-68.
4. H. Chi, C. Li, M. Huang, J. Wan, X. Zhou and B. Yan, *Chem. Eng. J.*, 2021, **424**, 130367.
5. J. R. Feng, Q. X. Deng and H. G. Ni, *Chemosphere*, 2022, **299**, 134475.
6. S. Yao, X. Li, H. Cheng, C. Zhang, Y. Bian, X. Jiang and Y. Song, *Bioresour. Technol.*, 2019, **293**, 122081.
7. M. W. Chang and J. M. Chern, *J. Hazard. Mater.*, 2009, **167**, 553-559.
8. T. Wei, D. Zhang, Z. Wang, Z. Zhou, T. Shumba, Y. Jiang, S. Zhuang, M. Cui, P. G. Ndungu, J. Tang, Z. Zhang and X. Qiao, *Chem. Eng. J.*, 2025, **504**, 158653.